DOI: 10.1002/chem.201300189

Solvent-Dependent Enantiodivergence in the Chlorocyclization of Unsaturated Carbamates

Atefeh Garzan,[a] Arvind Jaganathan,[a] Nastaran Salehi Marzijarani,[a] Roozbeh Yousefi,[a] Daniel C. Whitehead,[b] James E. Jackson,*[a] and Babak Borhan*[a]

Abstract: A remarkable solvent-controlled enantiodivergence is seen in the hydroquinidine 1,4-phthalazinediyl diether ((DHQD)$_2$PHAL)-catalyzed chlorocyclization of unsaturated carbamates. Eyring plot analyses of this previously unreported reaction are used to probe and compare the *R*- and *S*-selective pathways. In the $CHCl_3$/hexanes solvent system, the pro-*R* process shows a surprising increase in selectivity with increasing temperature. These studies point to a strongly solvent-dependent entropy–enthalpy balance between the pro-*R* and pro-*S* pathways.

Keywords: chlorocyclization · enantiodivergence · enantioselectivity · Eyring plots · organocatalysis · oxazolidinones

Introduction

The renaissance in asymmetric organocatalysis[1] seen in recent decades is largely the product of rational design based on mechanistic insights. Central to this progress has been the arsenal of analytical and theoretical tools enabling synthetic chemists to map out the factors that dictate structural and energetic preferences.[2] Some aspects of asymmetric catalysis, however, resist predictive design; a particularly challenging example is enantiodivergence, the uncommon situation in which a given chiral catalyst favors opposite enantiomers of a target product[3] as a function of reaction variables such as temperature, additives, or solvent. Of these parameters, the effect of solvent is perhaps the least predictable due to the variability of solute–solvent interactions.[4] Studies seeking to explain solvent-controlled enantiodivergent reactions have largely focused on temperature and solvent effects on catalyst conformations and additives that modulate substrate–catalyst interactions, factors expected to be pivotal in determining stereoselectivity.

Recently, a large body of work has appeared in the area of catalytic asymmetric halocyclization reactions.[5] In our own earlier reports on enantioselective alkene additions,[6] we described the catalytic asymmetric chlorocyclization of alkenoic acids[6c] and unsaturated amides.[6a] Turning to the unknown carbamate chlorocyclization reactions, we were surprised and delighted to uncover a solvent-dependent enantiodivergent chlorocyclization. Intriguingly, this enantiodivergence reflects differential entropy versus enthalpy contributions for the two enantiomeric pathways in different solvents. We report herein solvent, reagent, substrate, and temperature studies, along with NMR spectroscopic and Eyring plot analyses[7] to characterize these processes.

Results and Discussion

Discovery of the solvent-dependent enantiodivergence: The conversion of carbamate **1a** to oxazolidinone **2a** was studied with 1,3-dichloro-5,5-dimethyl hydantoin (DCDMH) as the chlorenium ion source in various solvents (Table 1). Pilot studies indicated that hydroquinidine 1,4-phthalazinediyl diether ((DHQD)$_2$PHAL; 10 mol%) was the best catalyst to promote formation of the desired oxazolidinone **2a**. In the course of solvent screening for this reaction, an intriguing trend emerged. The reaction of **1a** in aprotic solvents led to the formation of (*R*)-**2a** (Table 1, entries 1–5), with the highest stereoinduction observed in a 1:1 $CHCl_3$/hexanes solvent mixture (47% *ee*, Table 1, entry 4). In contrast, when the reaction was carried out in alcoholic solvents, (*S*)-**2a** was obtained (Table 1, entries 6–10), with *n*PrOH giving the highest *S* selectivity (−74% *ee*, Table 1, entry 9). The rough timescales of the reactions in the two media were similar (ca. 90 min to completion at −40°C), suggesting similar free-energy activation barriers to cyclization.

With solvents in hand to access either enantiomer, our efforts then focused on comparing the divergent mechanisms that select for *R* or *S* enantiomers. We initially hypothesized that the enantioselectivity switch might arise from differing catalyst conformations in different solvents. To explore this

[a] Dr. A. Garzan, A. Jaganathan, N. Salehi Marzijarani, Dr. R. Yousefi, Prof. J. E. Jackson, Prof. B. Borhan
Department of Chemistry, Michigan State University
East Lansing, MI 48824 (USA)
E-mail: jackson@chemistry.msu.edu
babak@chemistry.msu.edu

[b] D. C. Whitehead
Department of Chemistry, Clemson University
Clemson, SC 29634 (USA)

Supporting information for this article is available on the WWW under http://dx.doi.org/10.1002/chem.201300189.

Table 1. Solvent screen for the chlorocyclization reaction.

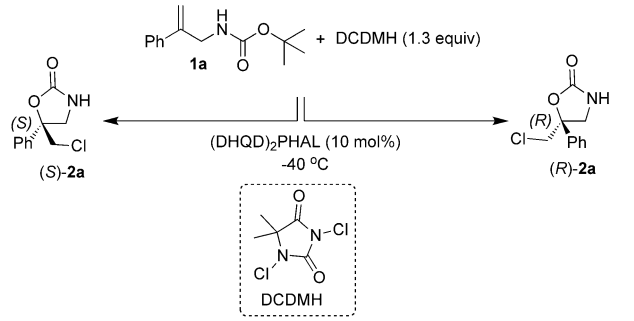

	Solvent	Product	Yield[a] [%]	*ee*[b] [%]
1	CH_2Cl_2	(*R*)-**2a**	93	+2
2	CH_3CN	(*R*)-**2a**	85	+14
3	$CHCl_3$	(*R*)-**2a**	79	+22
4	$CHCl_3$/hexanes[c]	(*R*)-**2a**	95	+47
5	$CHCl_3$/toluene[c]	(*R*)-**2a**	89	+43
6	TFE[d]	(*S*)-**2a**	94	−37
7	CH_3OH	(*S*)-**2a**	78	−36
8	C_2H_5OH	(*S*)-**2a**	79	−52
9	*n*PrOH	(*S*)-**2a**	88	−74
10	*n*BuOH	(*S*)-**2a**	86	−61

[a] Yields of the isolated product after column chromatography. [b] The *ee* values were determined by GC analysis; duplicate experiments found *ee* uncertainties of ±2%. [c] A 1:1 mixture. [d] 2,2,2-Trifluoroethanol.

Table 2. Halogen source screening.

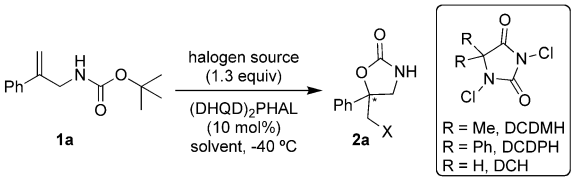

	Solvent	Halogen source	Yield[a] [%]	*ee*[b] [%]
1	$CHCl_3$/hexanes[c]	DCDMH	95	+47
2	$CHCl_3$/hexanes[c]	DCDPH	98	+46
3	$CHCl_3$/hexanes[c]	DCH	78	+28
4	$CHCl_3$/hexanes[c]	TCCA[d]	90	+21
5	$CHCl_3$/hexanes[c]	NCS[d]	57	0
6	*n*PrOH	DCDMH	88	−74
7	*n*PrOH	DCDPH[e]	NR	–
8	*n*PrOH	DCH	86	−70
9	*n*PrOH	TCCA[d]	90	−57
10	*n*PrOH	NCS[d]	51	−67
11[f]	*n*PrOH	DBDMH	90	−31
12[f]	*n*PrOH	NBS[d]	86	0

[a] Yields of the isolated product after column chromatography. [b] The *ee* values determined by GC analysis. [c] A 1:1 mixture. [d] TCCA = trichloroisocyanuric acid; NCS = *N*-chlorosuccinimide; NBS = *N*-bromosuccinimide. [e] DCDPH was not soluble under the reaction conditions; [f] Product is **2a'** with X=Br'; NR = no reaction.

supposition, NMR ROESY studies of the catalyst in deuterated methanol (as a surrogate for *n*PrOH) and in $CDCl_3$ were performed. In both solvents, contacts were found from H_d of the phthalazine ring to the quinoline H_c and to the quinuclidine moiety's ethyl group, indicating that the $(DHQD)_2PHAL$ catalyst adopts an open conformation (Figure 1). This assignment is further supported by the small

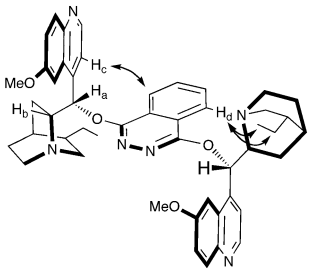

Figure 1. Structure of $(DHQD)_2PHAL$ in chloroform and methanol based on the NMR ROESY studies.

H_a to H_b coupling constant (<0.5 Hz in CD_3OD and $CDCl_3$), suggesting a dihedral angle close to 90 degrees.[8] These ROESY studies point to conformations of $(DHQD)_2PHAL$ that are similar in methanol and in chloroform. Having concluded that the free catalyst's solution-state conformations in protic and aprotic solvents are alike, we explored other variables to probe the factors affecting the observed enantiodivergent catalysis.

Exploration of factors that influence the enantiodivergence: The choice of halogen source strongly affected the enantioselectivity of the chlorocyclization of **1a**. In both $CHCl_3$/hexanes and *n*PrOH solvent systems, product *ee* values and/or yields (Table 2) were reduced by replacing DCDMH with other dichlorohydantoins, TCCA, NCS, or bromenium sources (NBS, 1,3-dibromo-5,5-dimethylhydantoin (DBDMH)). Given the negligible background reactions under these conditions, these results hint at an intimate association between the halenium source and the catalyst. The superior stereoselectivities obtained with halogenated hydantoins as opposed to other *N*-haloamines were consistent with our prior finding by NMR spectroscopy of a hydantoin–$(DHQD)_2PHAL$ interaction. Notably, however, all reagents studied retained the original findings' qualitative enantiopreferences for +*ee* in $CHCl_3$/hexanes and −*ee* in *n*PrOH.

In initial efforts to further optimize the stereoselectivity of this transformation, several carbamate substrates were studied. The variations in enantioselectivity with carbamate structure showed differing trends in the two solvent systems. Changing the *tert*-butyl group to a benzyl or cumyl group hardly affected the reaction's stereoselectivity in *n*PrOH (Table 3, entries 4–6). In $CHCl_3$/hexanes, however, the same changes to the carbamate structure eroded the stereoselectivity (Table 3, entries 1–3). This observation suggests that different modes of catalyst–substrate interaction are at play in the different solvents. It must be emphasized that enantioselectivity remained constant as a function of conversion in both solvents, supporting the notion of first-order participation of all reaction components.

Table 3. The effect of carbamate structure on enantioselectivity.

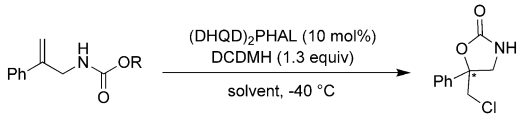

1a, R = *t*Bu **3a**, R = $C(CH_3)_2Ph$ **4a**, R = Bn

	Carbamate	Solvent	Yield[a] [%]	*ee*[b] [%]
1	**1a**	$CHCl_3$/hexanes	95	+47
2	**3a**	$CHCl_3$/hexanes	78	+25
3	**4a**	$CHCl_3$/hexanes	80	+13
4	**1a**	*n*PrOH	88	−74
5	**3a**	*n*PrOH	85	−73
6	**4a**	*n*PrOH	82	−71

[a] Yields of the isolated product after column chromatography. [b] The *ee* values were determined by GC analysis.

Basic and acidic additive screens by using substrate **1c** (see the Supporting Information, Tables S3 and S4) revealed that 0.5 equivalents of benzoic acid increase the selectivity of the chlorocyclization in *n*PrOH (−92% *ee* with benzoic acid vs. −74% *ee* without), but modestly erodes the selectivity in $CHCl_3$/hexanes. The effects of numerous additives are summarized in the Supporting Information; key findings are that in *n*PrOH the benzoic acid effect is not simply a matter of acidity; acetic and toluenesulfonic acids greatly reduced the reaction's enantioselectivity, reducing *ee* values to −20%, whereas citric acid had no discernible effect, yielding the product in −73% *ee*. Even in *n*PrOH, when the benzoic acid/catalyst ratio becomes too high, the stereoselectivity suffers. In contrast, bases such as triethylamine and imidazole destroy the enantioselectivity in both solvents. These findings suggest some differences between the *R*-selective and the *S*-selective chlorocyclization processes, but the general deleterious effects of both acids and bases (excluding benzoic acid) suggest that they may be disrupting catalyst–substrate hydrogen bonding that positions the substrate in the active site of the catalyst.

Substrate scope evaluation: With optimized conditions in hand, we examined the chlorocyclization of a series of substrates with substituted aryl groups on the olefin, as shown in Table 4. Aside from exploring the substrate scope for this new reaction, this exercise was undertaken to further map out the reactions' sensitivities to steric and electronic perturbations. For example, based on the findings given in Table 3, it was thought that changes in the substrates' steric parameters would more strongly affect enantioselectivities in $CHCl_3$/hexanes than in *n*PrOH. Indeed, the substrates in Table 4 gave consistently high enantioselectivity (−80 to −92% *ee*) in *n*PrOH, almost independent of the electron-rich/poor nature of the aryl substituent or of the steric bulk of the substituent. In sharp contrast, in the $CHCl_3$/hexanes solvent system, even small variations in the aryl substituent profoundly affected the reaction's enantioselectivity (+82 to −6% *ee*). Broadly speaking, the enantioselectivity progressively decreased with increasing steric bulk of the aryl ring

Table 4. Enantiodivergent chlorocyclization reactions.

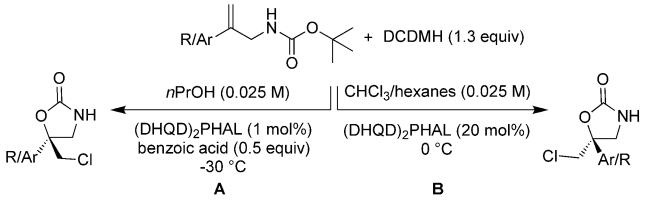

	Ar/R	Yield [%] (**A**)[a]	*ee* [%] (**A**)[b]	Yield [%] (**B**)[a]	*ee* [%] (**B**)[b]
1	C_6H_5 (**1a**)	87	−80	83	+82
2	4-F-C_6H_4 (**1b**)	92	−87	90	+75
3	4-Cl-C_6H_4 (**1c**)	98	−92	97	+65
4	4-Ph-C_6H_4 (**1d**)	86	−86	83	+50
5	4-Me-C_6H_4 (**1e**)	90	−82	86	0
6	4-CF_3-C_6H_4 (**1f**)	78	−80	80	+2
7	3,4-Cl-C_6H_3 (**1g**)	80	−88	81	+22
8	2,4,6-Me-C_6H_2[c] (**1h**)	58 (70)[d]	−83	40 (50)[d]	−6
9	$C_6H_5CH_2$ (**1i**)	87	−51	80	+65

[a] Yields of the isolated product after column chromatography. [b] The *ee* values were determined by GC or HPLC analysis. [c] In the presence of 2.0 equivalents of DCDMH. [d] The number in parentheses is the percentage conversion of the reaction.

(Table 4, entries 1–4), highlighting the importance of steric factors in the $CHCl_3$/hexanes medium. In contrast, electronic effects seem unimportant; the two isosteric, but electronically different, substituents 4-$CF_3C_6H_4$ and 4-$CH_3C_6H_4$ (Table 4, entries 5 and 6) gave practically no stereoinduction in $CHCl_3$/hexanes (+2% *ee* and 0% *ee*, respectively), suggesting that electronic factors play a negligible role in $CHCl_3$/hexanes. Replacement of the aryl moiety with a benzyl group gave better enantioselectivity in $CHCl_3$/hexanes than in *n*PrOH (+65% vs. −51% *ee*; Table 4, entry 9); this result stood out as the only one that significantly shifted the *ee* value in *n*PrOH, suggesting that the olefin's conjugation may be important in *n*PrOH whereas steric factors are more critical in $CHCl_3$/hexanes.

Chlorocyclization of **1c** showed significant temperature effects on the enantioselectivity. Specifically, selectivity for forming *S*-oxazolidinone **2c** in *n*PrOH decreased with increasing temperature (−74% *ee* at −40°C vs. −54% *ee* at 0°C). Conversely, and somewhat surprisingly, the same temperature increase improved the *R* selectivity in $CHCl_3$/hexanes (+20% *ee* at −40°C vs. +65% *ee* at 0°C). Thus, warmer temperatures favor the *R*-selective reactions in both media, broadly indicating a higher ΔH of activation for the *R*- than for the *S*-forming process. Having noted the similarity of the catalyst's conformation in alcoholic and chloroform media, we sought insight from the differential activation parameters associated with the diastereomeric transition states for the formation of the two enantiomers.

Eyring plot analyses to decipher the differential activation parameters: Based on their products' ease of analysis by GC and NMR spectroscopy, chlorocyclization of carbamates **1c** and **4c** were selected as test reactions for further studies. The absolute configuration of (*S*)-**2c** was verified by X-ray

diffraction and assumed to extend to the closely related aryl-ring-substituted analogues.[9] Cyclizations of **1c** and **4c** were performed with DCDMH in the presence of 20 mol% of the catalyst at various temperatures. This high catalyst loading was employed to ensure a negligible contribution from the small, but quantifiable, background reaction in $CHCl_3$/hexanes.[10] However, at high enough catalyst loading, enantiomer ratios remain constant as a function of reaction progress (as shown by quenching studies; see the Supporting Information, Table S7) and chlorinating agent concentration, suggesting similar molecularities for the pro-*R* and pro-*S* pathways and very slow background (uncatalyzed) reactions in either solvent system. These findings also point to negligible reaction inhibition by the products.

By using Eyring plot analyses of these studies (Figure 2), we hoped to address three important issues: first, to explain the trends in the temperature dependence of enantioselectivity in protic versus aprotic solvents; second, to explain the dependence (or lack thereof) of enantioselectivity on the carbamate substrates' structures in the two solvent systems; and third, on the basis of differential activation parameters obtained from the Eyring analysis, to gain insight into the substrate–catalyst–reagent–solvent interactions that invert the stereochemical preferences between the two solvent environments.

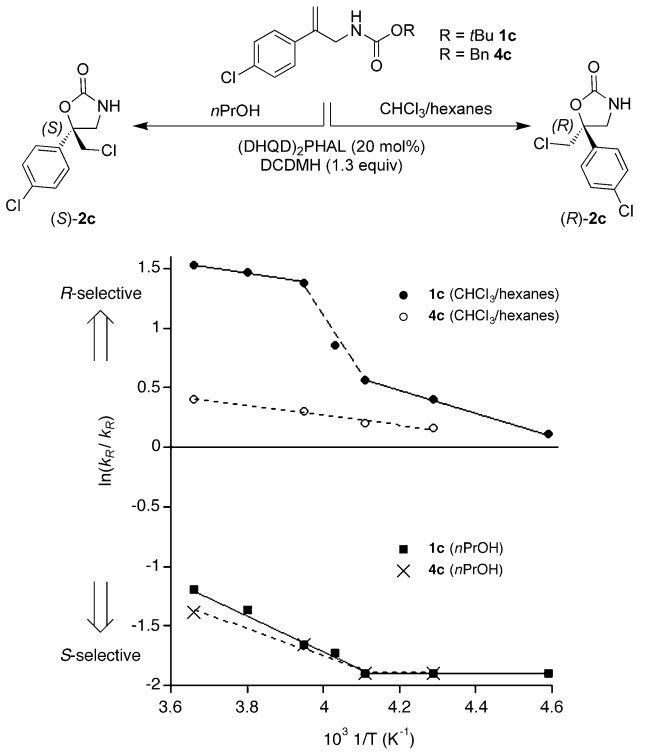

Figure 2. Eyring plots of ln[(100+% *ee*)/(100−% *ee*)] versus 1/T for chlorocyclization reactions (errors for each point were less than 2% of the value for each measurement).

If the competing cyclizations are interpreted as simple, one-step processes (an oversimplification, to be sure), the relative rates of formation of the *R* versus *S* product can be deduced from the relative yields. This notion is represented by Equation (1), in which $\Delta\Delta S^{\neq}_{R-S}$ and $\Delta\Delta H^{\neq}_{R-S}$ represent the differential activation entropy and enthalpy values for the respective *R*- and *S*-product-forming processes. As noted above, enantioselectivities (and hence, rate ratios) remain constant throughout the reactions in both solvent systems.

$$\ln(k_R/k_S) = -\Delta\Delta H^{\neq}_{R-S}/RT + \Delta\Delta S^{\neq}_{R-S}/\mathrm{R} \quad (1)$$

$$\Delta\Delta G^{\neq}_{R-S} = \Delta\Delta H^{\neq}_{R-S} - T\Delta\Delta S^{\neq}_{R-S} \quad (2)$$

The difference in the Gibbs free energy of activation for the formation of the two diastereomeric transition states can then be correlated to the differential activation enthalpy ($\Delta\Delta H^{\neq}_{R-S}$) and entropy ($\Delta\Delta S^{\neq}_{R-S}$) parameters. A more negative value for $\Delta\Delta G^{\neq}_{R-S}$ indicates a stronger preference for formation of the proto-*R* diastereomeric transition state over the alternative proto-*S* transition state. The sensitivity of the enantioselectivity to temperature reflects changes in the reactants' Boltzmann distributions and in the $\Delta\Delta G^{\neq}_{R-S}$ value (due to the $T\Delta\Delta S^{\neq}_{R-S}$ term) at different temperatures.

When the natural logarithms of the (*R*)-**2c**/(*S*)-**2c** product ratios obtained from Boc carbamate **1c** in *n*PrOH were plotted (black squares in Figure 2) versus reciprocal temperatures, two distinct straight-line segments emerged (Figure 2), with an inflection point at $T_{inf} = -30\,^{\circ}C$. From $-55\,^{\circ}C$ up to T_{inf}, the enantioselectivity is flat at its largest value (−74% *ee*), but then falls off as the temperature is raised further. Carbamate **4c** shows similar behavior (black crosses), with the inflection point at nearly the same location. Turning to the reaction of **1c** in 1:1 $CHCl_3$/hexanes, an analogous plot (black circles) showed two T_{inf} points, at −20 and $-30\,^{\circ}C$, resulting in two linear regions with different slopes and intercepts. The upper and lower extremities of the linear segments do not intersect; in the intervening region (denoted by the dotted line) the data point at $-25\,^{\circ}C$ was reproducible, but the inflections defining its endpoints are less well defined.[11] A similar Eyring plot analysis for chlorocyclization of the benzyl carbamate **4c** to (*R*)- and (*S*)-**2c** showed a single line (open circles), in contrast to **1c**. As noted earlier, higher temperatures led to higher *R* enantioselectivity in these cases.

Analysis of Eyring plot data: The nonlinear plots with their distinct inflection points suggest abrupt changes in mechanism or product-determining steps within narrow temperature ranges. Clearly, the simplified kinetic scheme implied by Equation (1), in which a single step controls each product's formation, is not sufficiently flexible to capture the behaviors shown in Figure 2. Instead, the kinked plots likely traverse kinetic "transitional regions" as discussed by Ridd et al., for which a switchover in rate-limiting steps occurs for each multistep enantiomer-forming process.[12] In the current system, this is manifested in temperature-dependent changes in the temperature dependence of the *R*/*S* ratio. The Eyring

plot analysis of relative rates extracts the differences between activation parameters of diastereomeric paths in the different temperature (and hence reaction mechanism) regimes.

The $\Delta\Delta G^{\neq}_{R-S}$ and resulting $\Delta\Delta H^{\neq}_{R-S}$ and $\Delta\Delta S^{\neq}_{R-S}$ values that can be calculated for the different linear segments in Figure 2 in $CHCl_3$/hexanes and in *n*PrOH are listed in Table 5, together with their relevant temperature regimes. It

Table 5. Differential enthalpy, entropy, and Gibbs free energy for the chlorocyclization reaction.[a,b]

	Solvent	Temp. [°C]	$\Delta\Delta H^{\neq}_{R-S}$ [kJ mol^{-1}]	$\Delta\Delta S^{\neq}_{R-S}$ [J mol^{-1} K^{-1}]	$\Delta\Delta G^{\neq}_{R-S}$ [kJ mol^{-1}][c]
1c	$CHCl_3$/Hex	−55→−30	8.0±0.6	37.8±2.6	–
1c	$CHCl_3$/Hex	−20→0	4.2±1.3	28.3±5.1	−3.5±1.9[e]
1c	*n*PrOH	−55→−30	0.0±0.6[d]	−15.8±2.6[d]	3.8±0.9[d,f]
1c	*n*PrOH	−30→0	13.1±1.2	38.0±4.8	–
4c	$CHCl_3$/Hex	−40→0	3.3±0.5	15.5±1.9	−0.9±0.7[e]
4c	*n*PrOH	−40→−30	−2.1±6.3	−24.6±26.7	–
4c	*n*PrOH	−30→0	9.6±2.8	23.7±10.9	3.8±3.9[f]

[a] Uncertainties for all values represent 95% confidence intervals by using the LINEST function in Microsoft Excel (Hex = hexanes). [b] Fitting each substrate/media dataset to a single line gives the following values: **1c**/CH_3Cl/hexanes: $\Delta\Delta H^{\neq}_{R-S}=14.6\pm3.1$, $\Delta\Delta S^{\neq}_{R-S}=66.6\pm12.5$; **1c**/*n*PrOH: $\Delta\Delta H^{\neq}_{R-S}=6.6\pm2.4$, $\Delta\Delta S^{\neq}_{R-S}=13.0\pm9.8$; **4c**/$CH_3Cl$/hexanes: $\Delta\Delta H^{\neq}_{R-S}=3.3\pm0.5$, $\Delta\Delta S^{\neq}_{R-S}=15.5\pm1.9$; **4c**/*n*PrOH: $\Delta\Delta H^{\neq}_{R-S}=7.2\pm2.7$, $\Delta\Delta S^{\neq}_{R-S}=14.8\pm10.9$; notably, uncertainties in the segments in the table above are generally smaller than those for the fully fitted datasets (except for **4c**/$CHCl_3$/hexanes, which already fits a single line). Together with visual inspection of Figure 2, these results validate division of the Eyring plots for all but **4c**/$CHCl_3$/hexanes into segments. [c] Negative values of $\Delta\Delta G^{\neq}_{R-S}$ favor the formation of the *R* enantiomer. For each substrate/media combination, the $\Delta\Delta G^{\neq}_{R-S}$ value shown is that calculated at the temperature of optimal selectivity. [d] These values represent a set of reactions that fortuitously gave exactly the same *ee* values; we infer uncertainties for this segment like those for **1c** in $CHCl_3$/hexanes in the same temperature regime. [e] $\Delta\Delta G^{\neq}_{R-S}$ was calculated at $T=0$°C (optimum temperature for highest *ee*). [f] $\Delta\Delta G^{\neq}_{R-S}$ was calculated at $T=-30$°C (optimum temperature for highest *ee*).

cannot be emphasized enough that these values represent differences between energy components for the pro-*R* and pro-*S* pathways, and not the absolute ($\Delta H^{\neq}$ and $\Delta S^{\neq}$) activation parameters controlling the reactions. Although the physical meaning of these $\Delta\Delta E$ quantities may be debated, a few interesting trends merit mention. For example, it is noteworthy that positive values are seen for $\Delta\Delta H^{\neq}_{R-S}$ for all of the transformations and temperature regimes in $CHCl_3$/hexanes and for all but the flat, low-temperature regions in *n*PrOH; thus formation of the *S* product is enthalpically preferred. This suggests that the pro-*S* pathway is more stabilized than the pro-*R* by favorable interactions among catalyst, substrate, and reagent. However, the *R* preference seen for the reaction of **1c** to form **2c** in $CHCl_3$/hexanes indicates that the stereoselectivity of the reaction is entropy driven (i.e., that the $-T\Delta\Delta S^{\neq}$ term overwhelms the positive $\Delta\Delta H^{\neq}$ term, resulting in an overall negative value for $\Delta\Delta G^{\neq}$), and thus becomes more predominant at warmer temperatures. Thus, the pro-*R* pathway may be understood to enjoy more degrees of freedom, which is consistent with the notion that the pro-*S* transition state is more tightly bound. This larger contrast between the pathways seems sensible in the less strongly solvating $CHCl_3$/hexanes medium. The transformation of **4c** into **2c** shows a similar, but much less pronounced, trend (compare open to filled circles in Figure 2). Not surprisingly, this enthalpy–entropy balance is sensitive to the steric impediments of the substrate, with the carboxybenzyl (CBz) carbamate giving lower enantioselectivities than the *tert*-butyloxycarbonyl (Boc) analogue.

For the *S*-selective behavior seen in *n*PrOH, the positive $\Delta\Delta H^{\neq}_{R-S}$ values exceed the smaller $-T\Delta\Delta S^{\neq}_{R-S}$ contributions, dictating the product stereoselectivity for transformation of both **1c** and **4c** into **2c**. These results suggest that the stabilizing interactions between substrate and catalyst that guide the reaction to the *S* product contribute significantly more in this case than differences in solvation or conformational degrees of freedom. This enthalpic control is most pronounced at lower temperatures. Experimental observations of the negligible effect of the carbamate bulk or aryl-ring substitution on the enantioselectivity of this reaction in *n*PrOH (see Table 2) suggest that the catalyst's complexation focuses around the reacting moieties (comparison of black crosses to black squares in Figure 2 shows very similar behavior of **1c** and **4c** in the temperature range evaluated in this study). However, the sharp transition to a plateau in enantioselectivity below −30°C is less easily rationalized.

Taken together, our results indicate that the solvent-dependent stereodiscrimination described herein is more likely guided by differential enthalpy versus entropy factors in the different media than by conformational changes in the catalyst. The enthalpy-controlled behavior in *n*PrOH suggests a strong interaction between carbamate and catalyst in the dominant diastereomeric transition state of the catalyzed chlorocyclization. On the other hand, the entropically controlled behavior of the reaction in $CHCl_3$/hexanes suggests a less constrained intermolecular interaction between the carbamate and catalyst. Yet this reaction's much greater sensitivity to structural perturbations might suggest a greater intimacy in the catalyst–substrate interaction. Gross reaction times also differ in their temperature sensitivity; reactions that run in approximately the same time in the two media at 0°C are much slower in $CHCl_3$/hexanes than in *n*PrOH at −30°C. Because of these seemingly contradictory findings, we are actively pursuing a more refined understanding of this rare solvent-dependent enantiodivergence with a focus on absolute activation parameters.

Conclusion

We present herein the first solvent-dependent enantiodivergent chlorocyclization of carbamates catalyzed by $(DHQD)_2PHAL$. This methodology enables selective access to both enantiomers of oxazolidinones by using a single chiral organocatalyst. Reaction characterization included exploration of variables including substrate structure, addi-

tives, solvent, and temperature. Eyring plot analyses suggest that enthalpy–entropy tradeoffs play a central role in the striking solvent-dependent stereodiscrimination seen in these reactions. Overall, increasing temperature favors formation of the *R* product in both media. The stereoselectivities of the *S*-selective cyclization in alcoholic solvents are dominated by variations in the enthalpies of activation ($\Delta\Delta H^{\neq}_{R-S}$), whereas $\Delta\Delta S^{\neq}_{R-S}$ governs the stereodiscrimination for the *R*-selective reaction in chloroform/hexanes. Further work to probe the mechanism of this rare enantioswitching process is underway and will be reported in due course.

Experimental Section

General procedure for the catalytic asymmetric chlorocyclization of carbamates in *n*PrOH: A screw-capped vial equipped with a stirring bar was charged with a stock solution of $(DHQD)_2PHAL$ (1.3 mL of 0.21 mg mL^{-1}) in *n*PrOH [0.30 mg $(DHQD)_2PHAL$, 1 mol%]. After cooling to −30 °C in an immersion cooler, DCDMH (9.5 mg, 0.041 mmol, 1.3 equiv) and benzoic acid (2.3 mg, 0.019 mmol, 0.5 equiv) were added sequentially. After stirring vigorously for 10 min, the substrate (0.037 mmol, 1.0 equiv) in *n*PrOH (0.2 mL, pre-cooled to the reaction temperature) was added in a single portion. The vial was capped and the stirring was continued at −30 °C until the reaction was complete, as judged by TLC (increasing the amount of DCDMH to 2.0 equivalents shortens the reaction time from 25 to 8 min (substrate **1a**) without affecting % *ee*). The reaction was quenched by the addition of aqueous NaOH (2%, 3 mL) and diluted with CH_2Cl_2 (3 mL). The organic compounds were separated and the aqueous layer was extracted with CH_2Cl_2 (3× 3 mL). The combined organic compounds were dried over anhydrous Na_2SO_4 and concentrated in the presence of a small quantity of silica gel. Pure products were isolated by column chromatography on a short silica gel column by using EtOAc/hexanes (1:4 to 1:1 gradient) as the eluent. Note: For reactions in 1:1 $CHCl_3$/hexanes, the catalyst loading was increased to 20 mol% to outcompete the background reaction at 0 °C. Furthermore, the acid additive was not included, however, the rest of the procedure was identical to those reported in the Supporting Information for $CHCl_3$/hexanes-mediated reactions.

Acknowledgements

The authors would like to thank Dr. R. J. Staples for the X-ray structure analysis, Mr. Jacob Matsil for assistance in the synthesis of some of the substrates, and the MSU Mass Spectrometry facility for HR-MS analysis. Generous support was provided by the NSF (CHE-0957462).

[1] *Comprehensive Asymmetric Catalysis* (Eds.: E. N. Jacobsen, A. Pfaltz, H. Yamamoto), Springer, Berlin, **1999**.
[2] a) G. Cainelli, D. Giacomini, P. Galletti, A. Quintavalla, *Eur. J. Org. Chem.* **2002**, 3153–3161; b) R. R. Knowles, S. Lin, E. N. Jacobsen, *J. Am. Chem. Soc.* **2010**, *132*, 5030–5032; c) Y. Sohtome, B. Shin, N. Horitsugi, R. Takagi, K. Noguchi, K. Nagasawa, *Angew. Chem.* **2010**, *122*, 7457–7461; *Angew. Chem. Int. Ed.* **2010**, *49*, 7299–7303.
[3] a) M. Bartók, *Chem. Rev.* **2010**, *110*, 1663–1705; b) Y. H. Kim, *Acc. Chem. Res.* **2001**, *34*, 955–962; c) M. P. Sibi, M. Liu, *Curr. Org. Chem.* **2001**, *5*, 719–755; d) T. Tanaka, M. Hayashi, *Synthesis* **2008**, 3361–3376; e) G. Zanoni, F. Castronovo, M. Franzini, G. Vidari, E. Giannini, *Chem. Soc. Rev.* **2003**, *32*, 115–129.
[4] a) G. Cainelli, P. Galletti, D. Giacomini, *Chem. Soc. Rev.* **2009**, *38*, 990–1001; b) G. Cainelli, D. Giacomini, P. Galletti, *Chem. Commun.* **1999**, 567–572; c) M. Messerer, H. Wennemers, *Synlett* **2011**, 499–502; d) Y. Sohtome, S. Tanaka, K. Takada, T. Yamaguchi, K. Nagasawa, *Angew. Chem.* **2010**, *122*, 9440–9443; *Angew. Chem. Int. Ed.* **2010**, *49*, 9254–9257; e) X. Tian, C. Cassani, Y. Liu, A. Moran, A. Urakawa, P. Galzerano, E. Arceo, P. Melchiorre, *J. Am. Chem. Soc.* **2011**, *133*, 17934–17941.
[5] a) A. Castellanos, S. P. Fletcher, *Chem. Eur. J.* **2011**, *17*, 5766–5776; b) J. Chen, L. Zhou, Y.-Y. Yeung, *Org. Biomol. Chem.* **2012**, *10*, 3808–3811; c) C. K. Tan, L. Zhou, Y. Y. Yeung, *Synlett* **2011**, *10*, 1335–1339; d) S. E. Denmark, M. T. Burk, *Org. Lett.* **2012**, *14*, 256–259; e) S. E. Denmark, M. T. Burk, A. J. Hoover, *J. Am. Chem. Soc.* **2010**, *132*, 1232–1233; f) S. E. Denmark, D. Kalyani, W. R. Collins, *J. Am. Chem. Soc.* **2010**, *132*, 15752–15765; g) M. C. Dobish, J. N. Johnston, *J. Am. Chem. Soc.* **2012**, *134*, 6068–6071; h) U. Hennecke, *Chem. Asian J.* **2012**, *7*, 456–465; i) D. Huang, H. Wang, F. Xue, H. Guan, L. Li, X. Peng, Y. Shi, *Org. Lett.* **2011**, *13*, 6350–6353; j) O. Lozano, G. Blessley, T. M. del Campo, A. L. Thompson, G. T. Giuffredi, M. Bettati, M. Walker, R. Borman, V. Gouverneur, *Angew. Chem.* **2011**, *123*, 8255–8259; *Angew. Chem. Int. Ed.* **2011**, *50*, 8105–8109; k) K. Murai, T. Matsushita, A. Nakamura, S. Fukushima, M. Shimura, H. Fujioka, *Angew. Chem.* **2010**, *122*, 9360–9363; *Angew. Chem. Int. Ed.* **2010**, *49*, 9174–9177; l) K. Murai, A. Nakamura, T. Matsushita, M. Shimura, H. Fujioka, *Chem. Eur. J.* **2012**, *18*, 8448–8453; m) R. J. Phipps, K. Hiramatsu, F. D. Toste, *J. Am. Chem. Soc.* **2012**, *134*, 8376–8379; n) S. A. Snyder, D. S. Treitler, A. P. Brucks, *Aldrichimica Acta* **2011**, *44*, 27–40; o) C. K. Tan, C. Le, Y.-Y. Yeung, *Chem. Commun.* **2012**, *48*, 5793–5795; p) C. K. Tan, L. Zhou, Y.-Y. Yeung, *Org. Lett.* **2011**, *13*, 2738–2741; q) G. E. Veitch, E. N. Jacobsen, *Angew. Chem.* **2010**, *122*, 7490–7493; *Angew. Chem. Int. Ed.* **2010**, *49*, 7332–7335; r) W. Zhang, N. Liu, C. M. Schienebeck, K. Decloux, S. Zheng, J. B. Werness, W. Tang, *Chem. Eur. J.* **2012**, *18*, 7296–7305; s) W. Zhang, S. Zheng, N. Liu, J. B. Werness, I. A. Guzei, W. Tang, *J. Am. Chem. Soc.* **2010**, *132*, 3664–3665; t) L. Zhou, J. Chen, C. K. Tan, Y.-Y. Yeung, *J. Am. Chem. Soc.* **2011**, *133*, 9164–9167; u) L. Zhou, C. K. Tan, X. Jiang, F. Chen, Y.-Y. Yeung, *J. Am. Chem. Soc.* **2010**, *132*, 15474–15476.
[6] a) A. Jaganathan, A. Garzan, D. C. Whitehead, R. J. Staples, B. Borhan, *Angew. Chem.* **2011**, *123*, 2641–2644; *Angew. Chem. Int. Ed.* **2011**, *50*, 2593–2596; b) D. C. Whitehead, M. Fhaner, B. Borhan, *Tetrahedron Lett.* **2011**, *52*, 2288–2291; c) D. C. Whitehead, R. Yousefi, A. Jaganathan, B. Borhan, *J. Am. Chem. Soc.* **2010**, *132*, 3298–3300; d) R. Yousefi, D. C. Whitehead, J. M. Mueller, R. J. Staples, B. Borhan, *Org. Lett.* **2011**, *13*, 608–611.
[7] H. Eyring, *J. Chem. Phys.* **1935**, *3*, 107–115.
[8] These results match those reported by Sharpless and co-workers in the asymmetric dihydroxylation reaction: H. C. Kolb, P. G. Andersson, K. B. Sharpless, *J. Am. Chem. Soc.* **1994**, *116*, 1278–1291.
[9] CCDC-890236 contains the supplementary crystallographic data for this paper. These data can be obtained free of charge from The Cambridge Crystallographic Data Centre via www.ccdc.cam.ac.uk/data_request/cif.
[10] Based on control experiments without the catalyst, at most a 2% yield could arise from the uncatalyzed background reaction by the time the catalyzed reaction is complete.
[11] Importantly, errors associated with individual data points (all triply replicated) were small relative to the large displacements among these segments.
[12] a) A minimal scenario that has the mathematical flexibility to show such behavior is one in which each path (pro-*R* and pro-*S*) consists of two sequential reactions, as discussed by Ridd et al (see below, refs. [12b,c]). Over the temperature range studied, these processes would trade roles as the rate-determining steps (RDS). This switch in RDS represents a change in the (kinetic) mechanism (although the sequence of events may be the same), and if the pro-*R* and pro-*S* switchover occurs at different temperatures, it allows for three regimes (i.e., slope segments) as seen in the Eyring plots in Figure 2. We cannot assign specific mechanistic events to its kinetic steps, nor rule out alternative multistep schemes. In future efforts to map out not only enantioselectivities, but also molecularity and absolute rates as a function of solvent, temperature, chlorinating agent, and substrate structures, we hope to develop a step-by-step mechanistic

understanding deep enough to allow predictive reaction design; b) K. J. Hale, J. H. Ridd, *J. Chem. Soc. Chem. Commun.* **1995**, 357–358; c) K. J. Hale, J. H. Ridd, *J. Chem. Soc. Perkin Trans. 2* **1995**, 1601–1605.

Received: January 18, 2013
Revised: March 19, 2013
Published online: May 13, 2013

